THE JOURNAL OF BIOLOGICAL CHEMISTRY VOL. 290, NO. 47, pp. 28272–28285, november 20, 2015

Cell Polarity Kinase MST4 Cooperates with cAMP-dependent Kinase to Orchestrate Histamine-stimulated Acid Secretion in Gastric Parietal Cells*

Received for publication, June 2, 2015, and in revised form, September 23, 2015 Published, JBC Papers in Press, September 24, 2015, DOI 10.1074/jbc.M115.668855

Hao Jiang[‡1], Wenwen Wang[‡§1], Yin Zhang[‡¶], William W. Yao[§2], Jiying Jiang[‡], Bo Qin[‡§3], Wendy Y. Yao[§2], Fusheng Liu[‡¶‖], Huihui Wu[‡§], Tarsha L. Ward[§], Chun Wei Chen[‡4], Lifang Liu[‖], Xia Ding[‡¶5], Xing Liu[‡§6], and Xuebiao Yao[‡7]

From the [‡]BUCM-USTC Joint Program in Cellular Dynamics and Anhui Key Laboratory for Cellular Dynamics, University of Science and Technology of China, Hefei 230027, China, the [¶]Beijing University of Chinese Medicine, Beijing 100029, China, the [§]Molecular Imaging Center, Atlanta Clinical and Translational Science Institute, Atlanta, Georgia 30310, and the [‖]Airforce General Hospital, Beijing 100036, China

Background: Polarized acid secretion in gastric parietal cells requires ezrin and its phosphorylation at Ser-66 by cAMP-dependent protein kinase (PKA).
Results: Phosphorylation of Ser-66 induces an ezrin conformational change that promotes the phosphorylation of Thr-567 by MST4.
Conclusion: PKA phosphorylates MST4 and ezrin to orchestrate histamine-elicited acid secretion.
Significance: The PKA-MST4-ezrin signaling axis is essential for parietal cell activation.

The digestive function of the stomach depends on acidification of the gastric lumen. Acid secretion into the lumen is triggered by activation of the PKA cascade, which ultimately results in the insertion of gastric H,K-ATPases into the apical plasma membranes of parietal cells. A coupling protein is ezrin, whose phosphorylation at Ser-66 by PKA is required for parietal cell activation. However, little is known regarding the molecular mechanism(s) by which this signaling pathway operates in gastric acid secretion. Here we show that PKA cooperates with MST4 to orchestrate histamine-elicited acid secretion by phosphorylating ezrin at Ser-66 and Thr-567. Histamine stimulation activates PKA, which phosphorylates MST4 at Thr-178 and then promotes MST4 kinase activity. Interestingly, activated MST4 then phosphorylates ezrin prephosphorylated by PKA. Importantly, MST4 is important for acid secretion in parietal cells because either suppression of MST4 or overexpression of non-phosphorylatable MST4 prevents the apical membrane reorganization and proton pump translocation elicited by histamine stimulation. In addition, overexpressing MST4 phosphorylation-deficient ezrin results in an inhibition of gastric acid secretion. Taken together, these results define a novel molecular mechanism linking the PKA-MST4-ezrin signaling cascade to polarized epithelial secretion in gastric parietal cells.

The functions of an epithelium depend on the polarized organization of its individual epithelial cells. The acquisition of a fully polarized phenotype and its plasticity control involve a cascade of complex events, including cell-cell adhesion, assembly of a lateral cortical complex, reorganization of the cytoskeleton, and polarized targeting of transport vesicles to the apical and basolateral membranes (1).

Ezrin is an actin-binding protein of the ezrin/radixin/moesin family of cytoskeleton-membrane linker proteins (2). Within the gastric epithelium, ezrin has been localized exclusively to parietal cells and primarily to the apical canalicular membrane of these cells (3, 4). Our previous studies have shown that gastric ezrin is co-distributed with the β-actin isoform *in vivo* (5) and preferentially bound to the β-actin isoform *in vitro* (6). It has been postulated that ezrin couples the activation of protein kinase A (PKA) to the apical membrane remodeling associated with parietal cell secretion (3, 7). In fact, we have mapped the PKA phosphorylation site on ezrin and demonstrated its functional importance in histamine-elicited gastric acid secretion (3). Using mouse genetics, Tamura *et al.* (8) have demonstrated that knocking down ezrin in stomachs to <5% of the wild-type levels results in severe achlorhydria. In these parietal cells, H,K-ATPase-containing tubulovesicles failed to fuse with the apical membrane, suggesting an essential role of ezrin in tubulovesicle docking. A recent study has shown that the levels of ezrin phosphorylation on Thr-567 are low in resting parietal cells and that histamine stimulation results in a slight increase of ezrin phosphorylation at Thr-567 (9). However, it was unclear how ezrin

* This work was supported by Chinese 973 Project Grant 2013CB911203; Ministry of Education Grant 20113402130010; Anhui Project Grant 08040102005; Chinese Natural Science Foundation Grants 31430054, 31271518, 31301105, 31501095, 90508002, and 90913016; National Institutes of Health Grants CA164133 and DK56292; China Postdoctoral Science Foundation Grant 2014M560517; and Central University Grants WK2340000032 and WK2340000021. The authors declare that they have no conflicts of interest with the contents of this article.
This study is dedicated to the late Professor John G. Forte, who discovered the essential role of ezrin in gastric acid secretion and founded the field of gastric parietal cell biology.
[1] Both authors contributed equally to this work.
[2] American Digestive Health Foundation student research fellow.
[3] Visiting scholar sponsored by the China Scholarship Council.
[4] Visiting student from Tsinghua University of Taiwan sponsored by the China Scholarship Council.
[5] To whom correspondence may be addressed. E-mail: dingx@bucm.edu.cn.
[6] To whom correspondence may be addressed. E-mail: xing1017@ustc.edu.cn.
[7] To whom correspondence may be addressed. E-mail: xyao@msm.edu.

phosphorylation of Thr-567 is orchestrated and whether it links to remodeling of the apical membrane and cytoskeleton during parietal cell activation.

Our studies demonstrate the functional significance of the vesicle trafficking machinery Stx3 (10), VAMP2 (11), and SNAP25 (12) in parietal cell secretion. Using atomic force microscopic analyses, we show that phosphorylation of Ser-66 unfolds the three compact lobes of the FERM (protein 4.1, ezrin, radixin, moesin) domain and that this conformational change enables association of Stx3 with ezrin (13). Our study provides novel insights into the spatial control of H,K-ATPase docking by phosphorylation-coupled ezrin-Stx3 interaction in parietal cells.

Mammalian MST4 kinase is a conserved element of the STE20 signaling cascade underlying cell polarity control (14). A recent study has shown that MST4 phosphorylates ezrin at Thr-567 at the apical membrane of intestinal cells, which induces brush borders (15). Here we show that MST4 is downstream from histamine-stimulated PKA activation and that activation of MST4 is important for parietal cell acid secretion by phosphorylation of Ser-66-phosphorylated ezrin. Therefore, our study provides novel insights into the PKA-MST4-ezrin signaling axis in polarized secretion in epithelial cells.

Materials and Methods

Isolation of Gastric Glands and Aminopyrine Uptake Assay—Gastric glands were isolated from New Zealand White rabbits as modified by Yao *et al.* (5). Briefly, the rabbit stomach was perfused under high pressure with PBS (2.25 mM K_2HPO_4, 6 mM Na_2HPO_4, 1.75 mM NaH_2PO_4, and 136 mM NaCl (pH7.4)) containing 1 mM $CaCl_2$ and 1 mM $MgSO_4$. The gastric mucosa was scraped from the smooth muscle layer, minced, and then washed twice with minimal essential medium buffered with 20 mM HEPES (pH7.4) (HEPES-minimal essential medium). The minced mucosa was then digested with 15 mg of collagenase (Sigma). Intact gastric glands were collected from the digestion mixture for 20–25 min and then washed three times in HEPES-minimal essential medium. In all subsequent gland experiments (AP[8] uptake assay), glands were resuspended at 5% cytocrit (v/v) in the appropriate buffer containing histamine receptor 2 blockers (cimetidine or famotidine, 5 μM) for the final assay.

Stimulation of intact and Streptolysin O (SLO)-permeabilized rabbit gastric glands was quantified using the AP uptake assay as described by Ammar *et al.* (16). Briefly, intact glands in HEPES-minimal essential medium were washed twice by settling at 4 °C in ice-cold K buffer (10 mM Tris base, 20 mM HEPES acid, 100 mM KCl, 20 NaCl, 1.2 mM $MgSO_4$, 1 mM NaH_2PO_4, and 40 mM mannitol (pH7.4)). SLO was added to a final concentration of 1 μg/ml, and the glands (at 5% cytocrit) were mixed by inversion and then incubated on ice for 10 min. The glands were then washed twice with ice-cold K buffer to remove unbound SLO, and the permeabilization was initiated by incubating the gland suspension at 37 °C in K buffer solution containing 1 mM pyruvate and 10 mM succinate.

The stimulation of intact gastric glands was achieved either by histamine (100 μM) plus IBMX (50 μM, Sigma) or using a membrane-permeable analog of cAMP, such as di-butyl cAMP (1 mM, Sigma) for different time intervals.

Cell Culture and Transfection—Primary cultures of gastric parietal cells from rabbit stomach were produced and maintained as described previously (3). Separate cultures of parietal cells were transfected with plasmids encoding GFP-tagged wild-type ezrin and/or mutants using Lipofectamine 2000 (Invitrogen) according to the instructions of the manufacturer. Briefly, 1 μg of DNA was incubated in 600 μl of Opti-MEM (antibiotic-free), whereas 6 μl of Lipofectamine 2000 was added and left at room temperature for 25 min. The cultured parietal cells (~3% cytocrit; 6-well plates) were washed once with Opti-MEM. The DNA-lipid mixture was added to the plates and incubated for 4 h, followed by replacement of 1.5 ml of medium B. The transfected cells were then maintained in culture at 37 °C until used for protein expression, partition, immunoprecipitation, or immunofluorescence.

Infection of cultured parietal cells with adenoviral mCherry-ezrin, mCherry-ezrin^{S66A}, mCherry-ezrin^{S66D}, mCherry-ezrin^{T567A}, mCherry-ezrin^{T567D}, mCherry-ezrin$^{S66A/T567D}$, and mCherry-ezrin$^{S66D/T567D}$ has been described previously (11–13). The infection efficiency and expression levels of various ezrin proteins exhibited no difference among different variants. MST4 siRNA, whose targeted sequence was the same as described previously (13), was synthesized by Qiagen.

Preparation of Gastric Subcellular Fractions—Gastric subcellular fractions were prepared according to Yao *et al.* (5). All fractionation procedures were performed under ice-cold conditions. Briefly, the treated glands were rinsed once in homogenizing buffer containing 125 mM mannitol, 40 mM sucrose, 1 mM EDTA, and 5 mM PIPES-Tris (pH 6.7) and homogenized with a very tightly fitting Teflon pestle. The homogenate was centrifuged to produce a series of pellets: P0, 40 × *g* for 5 min (whole cells and debris); P1, 4000 × *g* for 10 min (plasma membrane-rich fraction); P2, 14,500 × *g* for 10 min; P3, 100,000 × *g* for 60 min (microsomes); and S3, supernatant (cytosol). The pellets were resuspended in medium containing 300 mM sucrose, 0.2 mM EDTA, and 5 mM Tris (pH 7.4). The protein concentration in each individual subcellular fraction was assayed using bovine serum albumin as a standard (6).

Purification of Recombinant Ezrin Proteins—Recombinant wild-type ezrin, together with its phospho-mimicking (S66D) and non-phosphorylatable (S66A) mutants, was expressed in bacteria as hexahistidine-tagged proteins exactly as described previously (17). Purified ezrin was eluted with 250 mM imidazole and then applied to a gel filtration column to remove imidazole. The fusion protein was estimated to be of 90–95% purity as judged by SDS-PAGE. The major contaminants were degraded fragments of ezrin. Protein concentration was determined by Bradford assay.

[^{14}C]AP Uptake Assay—Stimulation of parietal cells was quantified using the AP uptake assay as described previously (18). Cells were transfected with siRNA 36 h before stimulation of histamine and IBMX (100 and 30 μM, respectively). AP uptake values were normalized among the various preparations by expressing them as a fraction of the stimulated control.

[8] The abbreviations used are: AP, aminopyrine; SLO, Streptolysin O; dbcAMP, di-butyl cAMP; IBMX, 3-isobutyl-1-methylxanthine.

Kinase Assay and in Vitro Phosphorylation—The kinase reactions were performed in 40 μl of 1× kinase buffer (25 mM HEPES (pH 7.2), 50 mM NaCl, 2 mM EGTA, 5 mM $MgSO_4$, 1 mM DTT, and 0.01% Brij35), casein, or various recombinant ezrin proteins (2 μg) as substrate, the catalytic subunit of PKA or purified MST4 (5–10 ng) as kinases, 5 μCi of [γ-^{32}P]ATP, and 500 μM ATP. Reaction mixtures were incubated at 30 °C for 30 min and then stopped by SDS sample buffer. Proteins were resolved by SDS-PAGE. Gels were dried and exposed, and the ^{32}P incorporation into casein proteins was quantified by PhosphorImager (Amersham Biosciences).

The kinetic parameters of MST4 were determined using the indicated concentrations of casein as substrates and 20 nM purified MST4 wild-type/mutants in the 20-μl phosphorylation mixture for 10 min. The amount of ADP produced from the kinase enzyme reaction was detected using the Amplite™ universal fluorimetric kinase assay kit (AAT Bioquest). MST4 phosphorylation was determined by measuring the phosphorylation in the presence of substrate and subtracted from the experiments in the absence of substrate. Data were fit to the Michaelis-Menten equation to derive apparent V_{max} and K_m with GraphPad Prism software.

Immunofluorescence Microscopy—Some cultured parietal cells were treated with 100 μM cimetidine to maintain a resting state. Others were treated with the secretory stimulants 100 μM histamine plus 50 μM IBMX in the presence of SCH28080, a proton pump inhibitor (3). Treated cells were then fixed with 2% formaldehyde for 10 min, washed three times with PBS, followed by permeabilization in 0.1% Triton X-100 for 5 min. Prior to application of primary antibody, the fixed and permeabilized cells were blocked with 0.5% BSA in PBS followed by incubation of primary antibodies against ezrin (4A5) and MST4, respectively. The endogenous ezrin proteins were labeled by a FITC-conjugated goat anti-mouse antibody and counterstained with MST4, which was labeled by rhodamine-conjugated goat anti-rabbit antibody. Coverslips were supported on slides by grease pencil markings and mounted in Vectashield mounting medium (Vector Laboratories).

Confocal Microscopy—Immunostained parietal cells were examined under a laser-scanning confocal microscope LSM510 NLO (Carl Zeiss, Germany) scan head mounted transversely to an inverted microscope (Axiovert 200, Carl Zeiss) with a 40× 1.0 numerical aperture PlanApo objective. Single images were collected at an average of 10 scans at a scan rate of 1 s/scan. Optical section series were collected with a spacing of 0.4 μm in the z axis through the ~12-μm thickness of the cultured parietal cells. The images from double labeling were collected simultaneously using a dichroic filter set with Zeiss image processing software (LSM 5, Carl Zeiss). Digital data were exported into Adobe Photoshop for presentation.

Western Blot Analysis—Samples were subjected to SDS-PAGE on a 6~16% gradient gel and transferred onto nitrocellulose membranes. Proteins were probed by appropriate primary antibodies and detected using ECL (Pierce). The band intensity was then quantified using a PhosphorImager (Amersham Bioscience).

Data Analyses—All fluorescence intensity measurements were carried out using MetaMorph software. The fluorescence intensities of various MST4 proteins at the apical membrane were determined by measuring the integrated fluorescence intensity within a 7 × 7 pixel square positioned over a single membrane ruffle and subtracting the background intensity of a 7 × 7 pixel square positioned in a region of cytoplasm lacking membrane ruffles. Maximal projected images were used for these measurements. The relative fluorescence intensity of various MST4 mutants at the apical membrane was calculated and expressed as ratio of MST4 signal over F-actin signal (stained by Alexa Fluor 647 phalloidin). To determine significant differences between means, unpaired Student's t tests assuming unequal variance were performed. Differences were considered significant at $p < 0.05$.

Results

Dynamic Phosphorylation of Ezrin during Parietal Cell Activation of Acid Secretion—Our early study showed that histamine stimulation of parietal cell acid secretion results in ezrin phosphorylation at Ser-66, which is sensitive to the PKA inhibitor H89, suggesting that phosphorylation of ezrin is a downstream event of PKA activity (3). Ser-66 of ezrin was then characterized as a substrate of PKA (13), which is essential for parietal cell activation via interacting with syntaxin 3 for tubulovesicle docking (19). Because a recent study has suggested that Thr-567 is also phosphorylated in histamine-stimulated parietal cell secretion, we sought to examine and compare the temporal profiles of Ser-66 and Thr-567 phosphorylation by Western blotting analyses using site-specific phosphorylation antibodies.

To delineate the molecular mechanisms underlying histamine-elicited ezrin phosphorylation in relation to specific sites of phosphorylation, we used histamine-stimulated gastric glands to measure the time course of ezrin phosphorylation judged by a Ser(P)-66 and a Thr(P)-567 antibody, respectively. Consistent with the literature (3), the protein level of ezrin did not change over time in response to histamine stimulation (Fig. 1*A*).

We next sought to examine the dynamics of Ser(P)-66 in response to histamine stimulation. A typical Western blot of Ser(P)-66 analyses is shown in Fig. 1*B*, demonstrating that the Ser(P)-66 signal reached a maximal level after about 15 min of stimulation and was sustained for 20 min. The quantitative index of Ser(P)-66 peaked at 10 min and slowly returned to near resting level by 35 min. The temporal profiles of ezrin protein phosphorylation at Ser-66 are consistent with the dynamics of parietal cell activation and reports in the literature (3).

To test whether the level of ezrin phosphorylation at Thr-567 is responsive to histamine stimulation, we used the aforementioned gastric gland samples to measure the time course of ezrin phosphorylation of Thr-567. A typical Western blot of Thr(P)-567 is shown in Fig. 1*C*, demonstrating that the Thr(P)-567 signal reached a maximal level after about 20 min of stimulation and was sustained for 20 min.

To compare the temporal dynamics of histamine-induced ezrin phosphorylation at Ser-66 with that of Thr-567, we carried out quantitative analyses of ezrin phosphorylation blots, shown in Fig. 1, *B* and *C*. The intensity of phospho-ezrin signals

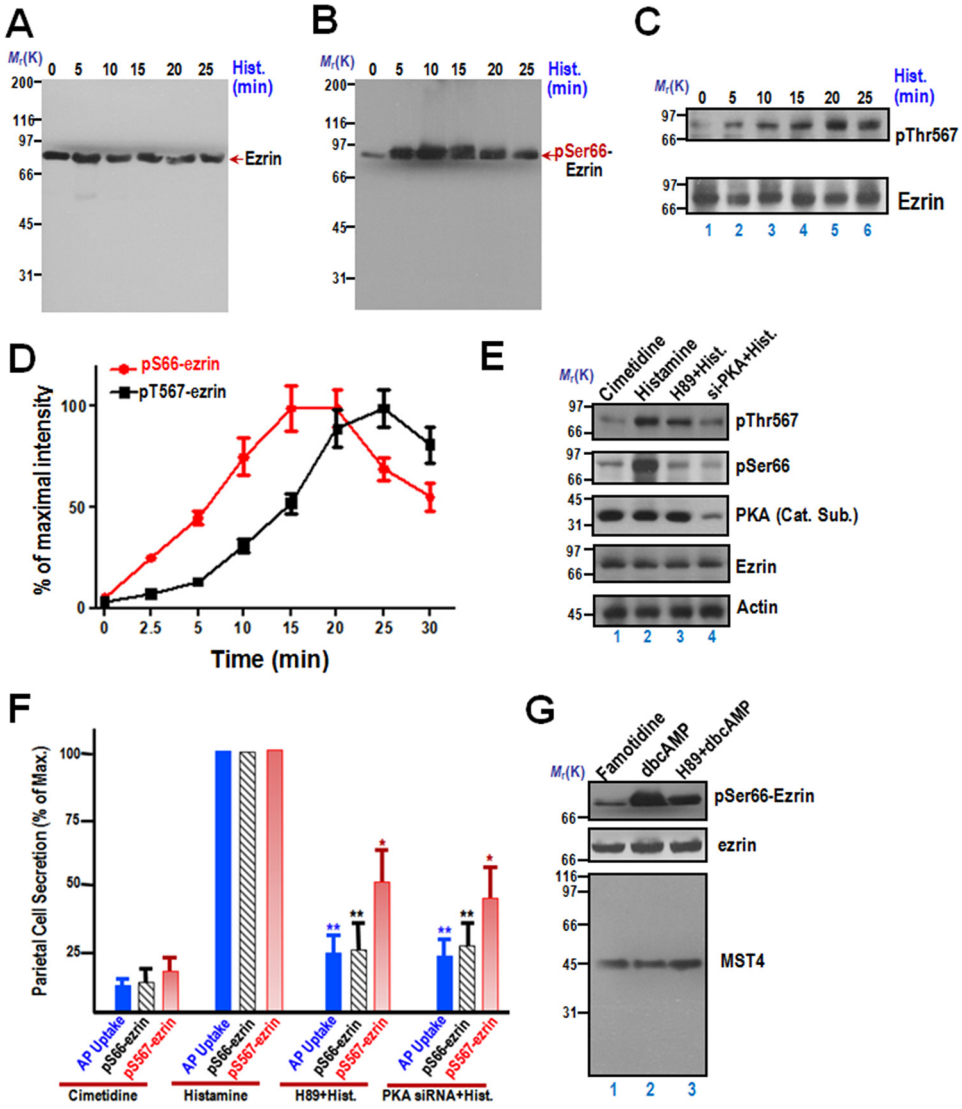

FIGURE 1. **Phosphorylation of ezrin at Ser-66 and Thr-567 exhibits distinct temporal dynamics during parietal cell activation.** *A*, aliquots of samples from resting and stimulated gastric glands were harvested at the indicated intervals after treatment as described under "Materials and Methods." The protein samples were separated by SDS-PAGE and transferred onto a nitrocellulose membrane. The nitrocellulose membrane was probed with the anti-ezrin mouse monoclonal antibody 6H11 as described previously (*e.g.* Refs. 3, 23). Note that the monoclonal antibody 6H11 is specific and recognizes essentially a single band at 80 kDa. *Hist.*, histamine. *B*, samples were prepared exactly as in *A*, and the membrane was probed with an anti-phospho-ezrin Ser-66 antibody (*pSer66*) and developed by ECL. Note that the anti-Ser(P)-66 antibody is specific and recognized essentially a single band at 80 kDa. *C*, samples were prepared exactly as in *A*, and the membrane was probed with an anti-phospho-ezrin Thr-567 antibody (*pThr567*) and developed by ECL. Another membrane from an identical preparation was probed with the anti-ezrin mouse antibody 6H11 as described previously. *D*, temporal profiles of ezrin phosphorylation at Ser-66 and Thr-567 of activated parietal cells. The stimulation index of Ser(P)-66 (*red line*) and Thr(P)-567 is expressed as phospho-ezrin intensities over that of ezrin protein from an identical set of samples. The stimulation index was also plotted as a function of time. *Error bars* represent the mean ± S.E. of three separate preparations. *E*, characterization of phospho-ezrin as a function of PKA activation. Western blots were probed with an anti-Thr(P)-567-ezrin antibody (*first panel*), anti-Ser (P)-66-ezrin antibody (*second panel*), the anti-PKA catalytic subunit (*Cat. Sub.*, *third panel*), anti-ezrin (*fourth panel*), and anti-actin antibody (*fifth panel*). *F*, correlation of the temporal dynamics of ezrin phosphorylation and acid secretion of parietal cells. The secretory activity of gastric glands was indicated by AP uptake and plotted as quantitative analyses of phosphorylated ezrin levels. *, $p < 0.05$; **, $p < 0.01$; significant difference from histamine-stimulated controls. *Max.*, maximal stimulation. *G*, aliquots of samples from resting and stimulated gastric glands were harvested at the indicated intervals after treatment as described under "Materials and Methods." Specifically, 5 μM famotidine and 1 mM dbcAMP were used to maintain gastric glands in a non-secreting and secreting status, respectively. In some instances, 10 μM H89 was incubated with an aliquot of gastric glands before dbcAMP treatment. After the aforementioned treatment, the protein samples were separated by SDS-PAGE and transferred onto a nitrocellulose membrane. The nitrocellulose membrane was probed with the anti-ezrin mouse monoclonal antibody 6H11 and Ser(P)-66 antibody as described above. In addition, the membrane was also probed by MST4 antibody as a control. Note that the anti-MST4 antibody from Cell Signaling Technology is specific and recognized essentially a single band at 43 kDa.

was compared with the resting control, normalized by ezrin protein intensity, and plotted (Fig. 1*D*). Typically, the relative acid secretory response reached a maximal level after about 15 min of stimulation and was sustained for the 35 min of measurement (3). The index of ezrin phosphorylation at Ser-66 peaked earlier, at about 10 min, and slowly returned to near resting level after 30 min (Fig. 1*D*, *red line*). On the other hand, the phosphorylation index for Thr-567 of ezrin reached its peak at about 20 min and was sustained beyond 30 min (Fig. 1*D*, *black line*). The temporal profiles of ezrin protein phosphorylation at Ser-66 and Thr-567 are consistent with reports in the literature (3, 7, 9) and suggest that the phosphorylation events of Ser-66 and Thr-567 may be coordinated for optimal parietal cell activation.

To examine whether phosphorylation of both Ser-66 and Thr-567 is a downstream event of PKA activation elicited by histamine, aliquots of cultured parietal cells were transiently transfected to introduce siRNA oligonucleotides for the catalytic subunit of PKA, followed by stimulation of histamine. Typically, siRNA treatment caused a 73.3% ± 8.1% suppression of the PKA catalytic subunit protein without altering the levels of other proteins, such as ezrin and actin (Fig. 1*E*, the *fourth* and *fifth panels*). Because the transfection efficiency in cultured parietal cells is around 75%, the siRNA-mediated reduction of 73% the catalytic subunit of PKA is considered "optimal." To avoid the possibility of the siRNA-mediated off-target effect and to provide an alternative measure to siRNA-elicited knockdown, we also included an aliquot of the PKA inhibitor H89 (10 μM). As shown in Fig. 1*E*, treatment of parietal cells with H89 did not alter the protein level of the PKA catalytic subunit (*third panel*). Consistent with the inhibition of PKA activity via either siRNA-mediated knockdown or pharmacological inhibition, the level of Ser(P)-66 is reduced dramatically judged by Western blot analysis (Fig. 3*E*, *second panel*, *lanes 3* and *4*). As shown in Fig. 1*F*, quantitative analyses indicated that treatment of H89 resulted in a 75.3% ± 6.7% reduction of ezrin phosphorylation at Ser-66, whereas siRNA treatment induced a typical 71.3% ± 9.8% reduction in Ser(P)-66 in histamine-stimulated preparations, which is consistent with reports in the literature (3, 7, 9).

We next examined the level of Thr(P)-567-ezrin in response to PKA knockdown and pharmacological inhibition. As shown in Fig. 1*E*, treatment of parietal cells with H89 resulted in a slight reduction in Thr(P)-567 level (*first panel*, *lane 3*), and suppression of PKA by siRNA also reduced the level of Thr(P)-567 (*first panel*, *lane 4*). Quantitative analyses indicated that treatment of H89 resulted in 71.3% ± 9.8% reduction of ezrin phosphorylation at Ser-66 but only a slight 45.3% ± 11.9% reduction in Thr(P)-567 level. The reduction in Thr(P)-567 level in the PKA siRNA-treated sample reached 53.7% ± 19.3%. To evaluate the histamine-induced ezrin phosphorylation in relation to activation of acid secretion, we plotted the acid secretion activity measured by AP uptake assay and compared it to levels of Ser(P)-66 and Thr(P)-567. As shown in Fig. 1*F*, the relative acid secretory response of parietal cells is a function of phosphorylation of Ser-66 and Thr-567. On the other hand, the index of Thr-567 phosphorylation is not as sensitive as that of Ser-66. Therefore, we reason that phosphorylation of Ser-66 and Thr-567 is essential for optimal parietal cell secretion.

To confirm that phosphorylation of Ser-66 elicited by histamine is a direct response to PKA activity and the level of Ser(P)-66 is low in histamine type 2 receptor-blocked parietal cells, aliquots of gastric gland samples were treated with famotidine (an alternative histamine type 2 receptor antagonist derived from cimetidine), di-butyl-cAMP (dbcAMP, a membrane-permeable cAMP analog), and H89 plus dbcAMP as described above, followed by Western blot analyses of the level of Ser(P)66-ezrin, ezrin, and MST4. As shown in Fig. 1*G*, the level of Ser(P)-66 in the famotidine-treated sample was minimal, whereas a stimulation of gastric glands with 1 mM dbcAMP resulted in a 6.3-fold increase in the level of Ser(P)-66 (*lane 2*). Consistent with early observations (Fig. 1*E*), PKA inhibition by H89 dramatically reduced the dbcAMP-elicited increase in Ser(P)-66 level (an approximately 61% reduction in Ser(P)-66 level; Fig. 1*G*, *lane 3*). Therefore, we conclude that the Ser(P)-66 level increase is a function of the activation of PKA in histamine-stimulated parietal cell secretion.

Phosphorylation of Ezrin at Thr-567 by MST4 Is Essential for Parietal Cell Acid Secretion—A recent study has shown that phosphorylation of ezrin at Thr-567 is essential for epithelial cell polarity establishment via MST4 phosphorylation (15). To test whether MST4 is also involved in parietal cell activation, we carried out ezrin immunoprecipitation using ezrin antibody-coupled affinity beads incubated with cell lysates from cimetidine-treated parietal cells and histamine-treated samples (13). As shown in Fig. 2*A*, MST4 from histamine-treated sample is greatly retained on ezrin affinity matrix (*center panel*, *lane 4*). MST4 from the cimetidine-treated sample was also found to associate with ezrin (Fig. 2*A*, *center panel*, *lane 3*), consistent with the report of MST4-ezrin interaction but less efficient (15).

To validate the relationship between MST4 and ezrin in gastric parietal cells, we carried out confocal microscopy analyses of their localization in isolated gastric glands. In permeabilized glands probed for ezrin (Fig. 2*B*, *a'*), parietal cells exhibit intense staining of an intracellular network reminiscent of the apical plasma membrane that is sequestered in the form of the intracellular canaliculi (*arrows*). MST4 is primarily localized to cytoplasm of parietal cells containing ezrin (Fig. 2*B*, *b'*). A series of optical sections were taken from identical planes for glands probed simultaneously for ezrin and MST4. Both ezrin and MST4 are absent from the non-parietal cells. In parietal cells, ezrin exhibits primarily characteristics of the tortuous apical canalicular surface wending through most of the cell, whereas MST4 shows a relatively light deposition of stain at the apical canalicular surface (Fig. 2*B*, *c'*).

To examine whether phosphorylation of Thr-567 is a downstream event of MST4 activation elicited by histamine, aliquots of cultured parietal cells were transiently transfected to introduce siRNA oligonucleotides for MST4, followed by stimulation of histamine. Typically, siRNA treatment caused a 79.3% ± 5.1% suppression of MST4 protein without altering the levels of other proteins, such as ezrin and the catalytic subunit of PKA (Fig. 2*C*, *second* and *fifth panels*). As shown in Fig. 2*C*, suppression of MST4 via siRNA-mediated knockdown resulted in a dramatic reduction of Thr(P)-567, as judged by Western blot analysis (*fourth panel*). Quantitative analyses indicated that suppression of MST4 via siRNA-mediated knockdown resulted in a 73.7% ± 9.3% reduction of ezrin phosphorylation at Thr-567 without a significant reduction in Ser(P)-66 level in histamine-stimulated preparations (Fig. 2*D*), suggesting that MST4-elicited phosphorylation of Thr-567 is a downstream event of PKA activation.

To probe for the requirement of MST4 in parietal cell acid secretion in response to histamine stimulation, we carried out an AP uptake assay in MST4 siRNA-treated and scramble-transfected parietal cells, as described previously (19, 20). As shown in Fig. 2*E* (*red columns*), suppression of MST4 by siRNA treatment resulted in an inhibition of 51.3% ± 9.7% in acid secretion, as judged by AP uptake (*, $p < 0.05$), suggesting that MST4 is essential for parietal cell acid secretion. As a positive

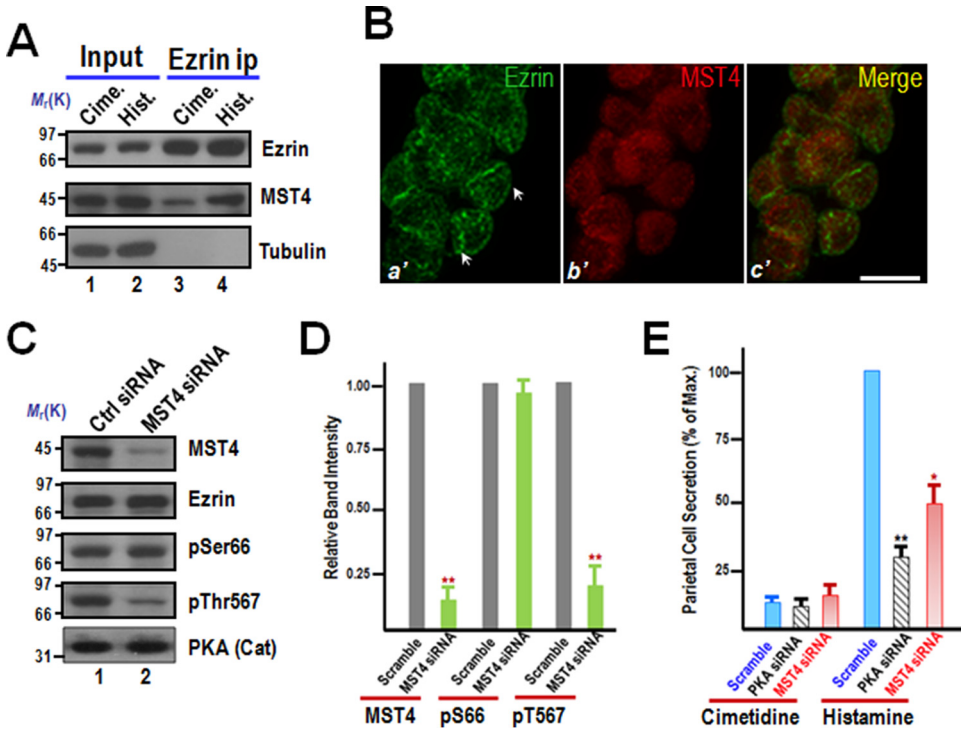

FIGURE 2. **MST4 is essential for gastric parietal cell acid secretion elicited by histamine.** *A*, phosphorylation of Ser-66 of ezrin promotes its association with MST4. Parietal cell lysates from cimetidine (*Cime*)- and histamine (*Hist*)-stimulated samples were clarified and incubated with ezrin affinity matrix. Beads were washed and boiled in SDS-PAGE sample buffer, followed by Western blot analyses of proteins bound to the beads. Note that a higher level of MST4 was immunoprecipitated by ezrin antibody from the secreting parietal cell fraction. *B*, MST4 specifically localizes to gastric parietal cells. Double immunofluorescence microscopic analyses show the co-existence of ezrin and MST4 in parietal cells using isolated gastric glands from rabbit. *Scale bar* = 10 μm. *C*, MST4 is responsible for Thr-567 phosphorylation during acid secretion by histamine stimulation. Aliquots of cultured parietal cells were transfected to introduce MST4 siRNA and control oligonucleotide. 24 h after transfection, parietal cells were stimulated with 100 μM histamine plus 50 μM IBMX for 20 min, and then cell lysates were generated and clarified for Western blot analyses of MST4 knockdown efficiency and its impact on ezrin phosphorylation. Note that MST4 was suppressed by siRNA treatment, which did not change the level of Ser(P)-66 but suppressed the level of Thr(P)-567. *Ctrl*, control. *D*, quantification of the level of MST4, Ser(P)-66-ezrin, and Thr(P)-567-ezrin in parietal cells treated with MST4 siRNA. The control experiment was done using a scrambled oligonucleotide or irrelevant siRNA. *Error bars* represent the mean ± S.E. of three separate preparations. **, $p < 0.01$ compared with the scramble siRNA-transfected control. *E*, MST4 is essential for parietal cell acid secretion. Aliquots of cultured parietal cells were transfected with MST4 and PKA (catalytic subunit) siRNA and scrambled oligonucleotides, followed by a standardized AP uptake assay. **, $p < 0.01$; *, $p < 0.05$ compared with stimulated controls. *Max.*, maximal stimulation. *Error bars* represent the mean ± S.E. of three separate preparations.

control, suppression of PKA by siRNA treatment resulted in an inhibition of 78.5% ± 5.1% in acid secretion, as judged by AP uptake (Fig. 2*E*, *black bars*; **, $p < 0.01$). Therefore, we conclude that MST4 is essential for parietal cell acid secretion in histamine stimulation.

PKA Phosphorylates MST4 and Promotes Its Kinase Activity—Our recent study has demonstrated that phosphorylation of Ser-66 opens the compact lobes, which enables its association with syntaxin 3 (13), which enables the docking of tubulovesicle for proton pump insertion at the apical membrane. The requirement of MST4 for acid secretion and the phosphorylation of ezrin at Thr-567 by MST4 prompted us to examine the regulation of MST4 by PKA.

Our computational analyses of the PKA phosphorylation site suggested Thr-178 of MST4 as a potential site for the PKA substrate. Thr-178 is located at the kinase domain of MST4 (Fig. 3*A*). To test whether Thr-178 of MST4 is a substrate of PKA, we performed *in vitro* phosphorylation on hexahistidine-tagged MST4 proteins, including both wild-type MST4 and a mutant MST4 in which threonine 178 was replaced by alanine (T178A). Both hexahistidine-tagged proteins, the wild type, and the Thr-178-mutated MST4 mutant ($MST4^{T178A}$) migrate at about the predicted 45 kDa, as shown in Fig. 3*B* (*top panel*, Coomassie Blue stain). Incubation of the fusion proteins with [γ-^{32}P]ATP and the catalytic subunit of PKA resulted in the incorporation of ^{32}P into wild-type but not T178A mutant MST4 (Fig. 3*B*, *bottom panel*, *lane 3*). This PKA-mediated phosphorylation is specific because incubation of MST4 with [γ-^{32}P]ATP in the presence of the PKA inhibitor H89 resulted in no detectable incorporation of radioactivity into the wild-type protein (Fig. 3*B*, *lane 1*). Quantitative analyses show that incorporation of ^{32}P into MST4 is a function of PKA (Fig. 3*C*). Therefore, Thr-178 of MST4 is a substrate for PKA.

To delineate how PKA phosphorylation results in regulation of MST4 kinase activity, we carried out enzymatic activity assays comparing the kinetic parameters of recombinant MST4 wild-type ($MST4^{WT}$), kinase-dead (K53R, $MST4^{K_D}$), phospho-mimicking mutant ($MST4^{T178D}$), and non-phosphorylatable mutant ($MST4^{T178A}$) using casein and ATP as substrates. The initial velocities of MST4 and its phospho-mimicking and non-phosphorylatable mutants were measured at various concentrations of the substrate casein, whereas the concentration of ATP was fixed. The kinetics data were plotted in the Michaelis-Menten format with velocity *versus* concentration of casein (Fig. 3*D*) and in the double reciprocal format with 1/velocity *versus* 1/concentration of casein (Fig. 3*E*). As the analyses by

double-reciprocal plot shown in Fig. 3*E*, the maximal velocity of phosphorylation by $MST4^{T178A}$ was about 8.5-fold slower compared with that of $MST4^{T178D}$. On the basis of a Lineweaver-Burk analysis, the calculated K_m was 3.7 ± 1.8 for K178A and 0.93 ± 0.2 for the T178D mutant. The calculated k_{cat}/K_m, an indicator for catalytic efficiency, for T178D is 69.8, whereas the k_{cat}/K_m, for T178A is 4.3. The enzymatic analyses indicate that phosphorylation of MST4 by PKA not only promoted the catalytic rate but also increased the affinity between MST4 and its substrates.

We next examined whether PKA phosphorylation modulates the catalytic activity of MST4 using ATP as a substrate. As shown in Fig. 3*G*, the calculated k_{cat}/K_m for T178D was 22.6, whereas the k_{cat}/K_m for T178A was 1.4. The k_{cat}/K_m for the kinase-deficient mutant MST4 is 0.4. These kinetic analyses indicate that phosphorylation of MST4 by PKA at Thr-178 not only promoted the catalytic rate but also increased the affinity between MST4 and ATP. Therefore, we conclude that PKA phosphorylation of MST4 promotes the activity of MST4 to catalyze phosphate transfer to its substrates.

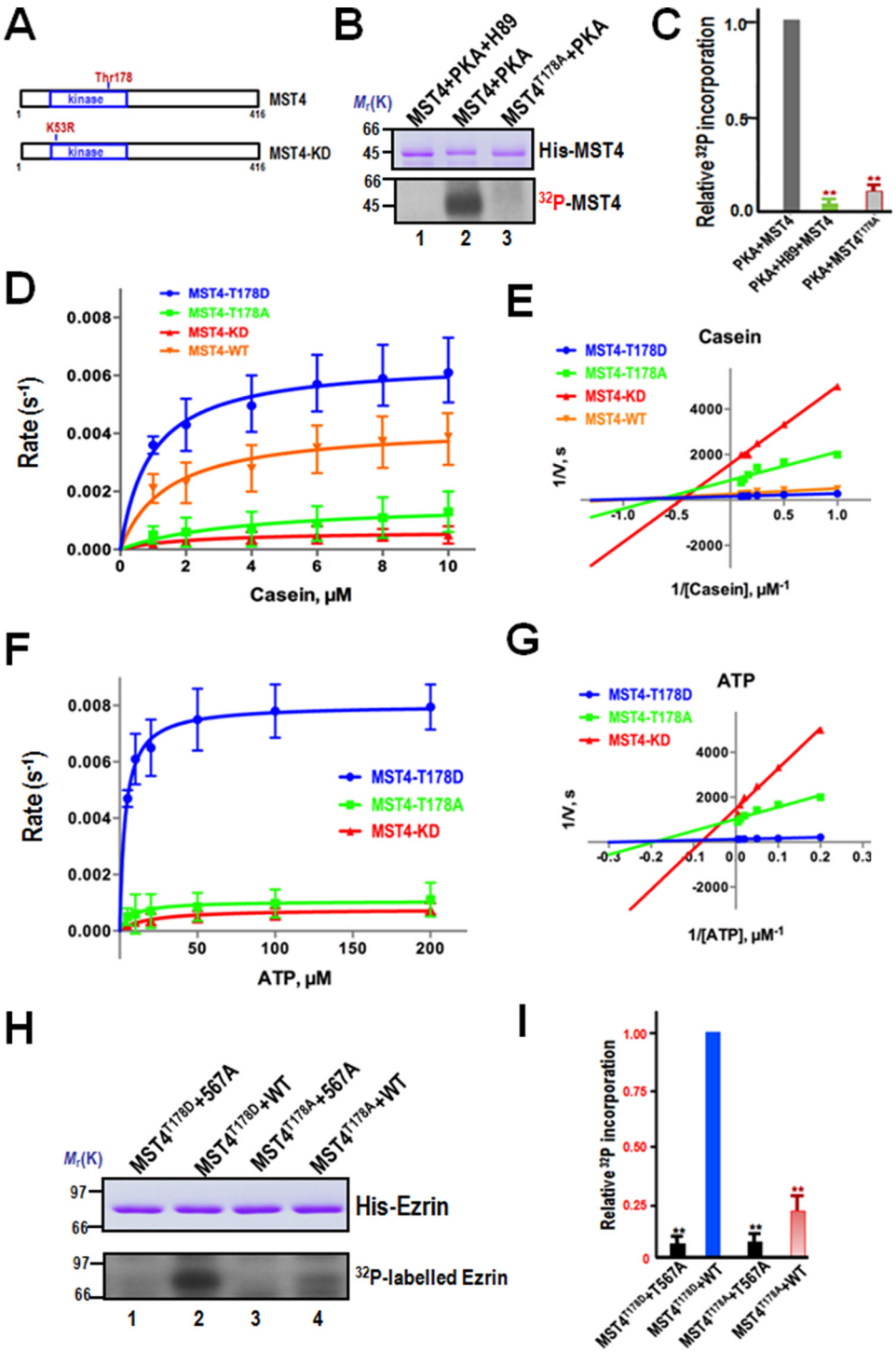

To validate whether MST4^{T178D} exhibits much greater efficiency in phosphorylating ezrin compared with MST4^{T178A}, we performed *in vitro* phosphorylation on hexahistidine-tagged ezrin proteins, including both wild-type ezrin and a mutant ezrin in which threonine 567 was replaced by alanine (T567A). Both hexahistidine-tagged proteins, wild-type and T567A, migrate at about the predicted 80 kDa, as shown in Fig. 3*H* (*top panel*, Coomassie Blue stain). Incubation of the fusion proteins with [γ-^{32}P]ATP and the MST4^{T178D} recombinant protein resulted in the incorporation of ^{32}P into wild-type but not T567A mutant ezrin (Fig. 3*H*, *bottom panel*, *lanes 1* and *2*). As predicted, the MST4^{T178A} version retained a little catalytic activity toward wild-type but not T567A mutant ezrin (Fig. 3*F*, *bottom panel*, *lanes 3* and *4*). Quantitative analyses indicate that MST4^{T178D} exhibits about 4.1-fold greater efficiency in the phosphorylation of ezrin compared with MST4^{T178A} (Fig. 3*I*). Therefore, we conclude that activation of PKA elicits a phosphorylation of MST4 that promotes the phosphorylation of ezrin at Thr-567 during parietal cell activation of acid secretion.

MST4 Phosphorylation of Thr-567 Is Amplified by Phosphorylation of Ser-66 by PKA—The crystal structure reveals that the FERM domain has three compact lobes in which Ser-66 resides. We speculate that phosphorylation of Ser-66 opens the compact lobes, which enables its release of the intramolecular N-C association (20). To test this hypothesis, we performed *in vitro* phosphorylation on recombinant ezrin fusion proteins, including both wild-type and mutant ezrin proteins (S66A and S66D). As shown in Fig. 4*A*, the hexahistidine-tagged proteins, wild type, S66A, and S66D, migrate at about the predicted 80 kDa, as shown in Fig. 4*A* (*top panel*, Coomassie Blue stain). Incubation of the fusion proteins with [γ-^{32}P]ATP and the MST4 recombinant protein resulted in the incorporation of ^{32}P into wild-type and S66D but not S66A mutant ezrin (Fig. 4*A*, *center panel*, *lanes 1* and *2*). Western blot analysis with anti-phospho-ezrin Thr-567 antibody confirmed the phosphorylation of Thr-567 on wild-type and S66D ezrin (Fig. 4*A*, *bottom panel*, *lanes 1* and *2*). Quantitative analyses indicate that S66D ezrin exhibits an approximately 4.5- and 9.3-fold greater efficiency in ^{32}P incorporation compared with the wild type and S66D, respectively (Fig. 4*B*). Therefore, we conclude that PKA phosphorylation of ezrin at Ser-66 promotes the phosphorylation of ezrin at Thr-567 by MST4.

Because parietal cell activation involves ezrin-mediated reorganization of the apical membrane cytoskeleton, we sought to probe the localization of MST4 using immunofluorescence microscopy. As shown in Fig. 4*C*, *a'*, MST4 is primarily localized to the cytoplasm of parietal cells treated with cimetidine. However, MST4 is enriched in the apical membrane in histamine-stimulated parietal cells (Fig. 4*C*, *b'*).

To evaluate the role of PKA-elicited phosphorylation of MST4 in parietal cell activation, we attempted to transiently transfect cultured parietal cells for expressing exogenous MST4. To test the efficiency of exogenous MST4 expression, cultured parietal cells were transfected with GFP-tagged wild-type and mutant MST4 plasmids. Western blot analysis carried out using transfected cells showed that exogenously expressed MST4 proteins were about 2.5- to 3-fold higher than the level of endogenous ezrin in cultured parietal cells (Fig. 4*D*). Assuming a transfection efficiency of about 55–60%, the actual expression level of GFP-MST4 in positively transfected cells is about 4-fold higher than that of endogenous protein.

Because parietal cell activation is hallmarked by the translocation of H,K-ATPase from tubulovesicles to the apical membrane, we sought to assess the parietal cell activation in phospho-mimicking MST4 (GFP-MST4^{T178D})- and non-phosphorylatable MST4 (GFP-MST4^{T178A})-expressing cells. The transfected cells were then treated with either cimetidine or histamine before being fixed for immunofluorescence microscopy analyses. As shown in Fig. 4*E*, although GFP-MST4^{T178A} is primarily localized to the cytoplasm of cimetidine-treated cells (*a'*), it becomes relocated to the apical plasma membrane in response to histamine stimulation (*b'*). Consistent with our speculation, expression of phospho-mimicking MST4 (MST4^{T178D}) resulted in an expansion of the apical

FIGURE 3. **PKA-elicited phosphorylation of Thr-178 promotes MST4 kinase activity.** *A*, schematic of the MST4 structure with annotation of the putative PKA substrate site Thr-178. The kinase-dead MST4 (*K53R*) is also illustrated. *B*, Thr-178 of MST4 is a substrate of PKA *in vitro*. Aliquots of recombinant hexahistidine-tagged MST4 were purified and incubated with PKA and PKA plus the pharmacological inhibitor H89 as detailed under "Materials and Methods." As a control, an aliquot of recombinant MST4 with the putative PKA site mutated to alanine (*MST4^{T178A}*, *lane 3*). Top panel, Coomassie Blue-stained SDS-PAGE. *Bottom panel*, ^{32}P incorporation from the same gel. *C*, quantitative analyses of *in vitro* phosphorylation efficiency. **, $p < 0.01$ compared with stimulated controls. *Error bars* represent the mean ± S.E. of three separate preparations. *D*, PKA phosphorylation-elicited MST4 enzymatic kinetics in response to increased concentrations of substrate casein. The MST4 concentration is 20 nM. The Michaelis-Menten data of MST4 activity at various concentrations of substrate casein are shown. *Error bars* represent the mean ± S.E. of three separate preparations. The *orange line* with *inverted triangles* represents the kinetics of wild-type MST4. The *red line* with *upright triangles* represents the kinase-deficient mutant. The phospho-mimicking mutant is shown as a *blue line* with *dots*, and the non-phosphorylatable mutant is marked by a *green line* with *squares*. *E*, Lineweaver-Burk plot of *D*. Lineweaver-Burk analysis is an efficient method of linearizing substrate-velocity data to determine the kinetic constants $K_m$and V_{max}. On the basis of Lineweaver-Burk analysis, the calculated K_m was derived for wild-type MST4 (1.5 ± 0.4), the kinase-deficient mutant (2.1 ± 0.4), the T178A mutant (3.7 ± 1.8), and the T178D mutant (0.93 ± 0.2). The calculated k_{cat}/K_m, an indicator for catalytic efficiency, for T178D is 69.8 whereas the k_{cat}/K_m for T178A is 4.3. The k_{cat}/K_m, for wild-type MST4 is 29.3. The kinetic analyses indicate that phosphorylation of MST4 at Thr-178 promotes its kinase activity using casein as a substrate. *F*, PKA phosphorylation-elicited MST4 enzymatic kinetics in response to increased concentrations of substrate ATP. The Michaelis-Menten data of MST4 activity at various concentrations of ATP are shown. The MST4 concentration is 20 nM. *Error bars* represent the mean ± S.E. of three separate preparations. The *red line* with *upright triangles* represents the kinase-deficient mutant. The phospho-mimicking mutant is shown as a *blue line* with *dots*, and the non-phosphorylatable mutant is marked by a *green line* with *squares*. *G*, Lineweaver-Burk plot of *F*. On the basis of Lineweaver-Burk analysis of MST4 kinetics in the presence of ATP, the calculated K_m was derived for the kinase-deficient mutant (18.5 ± 5.2), T178A mutant (7.6 ± 1.9), and T178D mutant (3.6 ± 0.3). The calculated k_{cat}/K_m, an indicator for catalytic efficiency, for T178D is 22.6, whereas the k_{cat}/K_m for T178A is 1.4. The k_{cat}/K_m for the kinase-deficient mutant MST4 is 0.4. The kinetic analyses indicate that phosphorylation of MST4 at Thr-178 promotes its efficiency in using ATP as a substrate. These kinetic analyses indicate that phosphorylation of MST4 by PKA not only promoted the catalytic rate but also increased the affinity between MST4 and ATP. *H*, PKA phosphorylation-mimicking MST4 exhibits better efficiency in phosphorylation of ezrin *in vitro*. Aliquots of recombinant hexahistidine-tagged ezrin, including the wild type and ezrin mutant (T567A), were incubated with MST4 and the PKA phosphorylation-mimicking mutant MST4^{T178A}, as detailed under "Materials and Methods." *Top panel*, Coomassie Blue-stained SDS-PAGE. *Bottom panel*, ^{32}P incorporation from the same gel. *I*, quantitative analyses of *in vitro* phosphorylation efficiency of Thr-567 by MST4. **, $p < 0.01$ compared with stimulated controls. *Error bars* represent the mean ± S.E. of three separate preparations.

membrane in parietal cells (Fig. 4*E*, *c'*) because the majority of MST4^{T178D} is concentrated at the apical membrane of parietal cells. MST4^{T178D}-expressing cells produce a characteristic vacuolar swelling in response to histamine stimulation (Fig. 4*E*, *d'*), suggesting the potential role of MST4 activation in recruiting H,K-ATPase-containing vesicles to the apical membrane. Quantitative analyses demonstrate that MST4 is relocated to the apical membrane in response to histamine stimulation (Fig. 4*F*). Previous studies have revealed that vacuole diameter can be used as a reporter for parietal cell secretory activity (13).

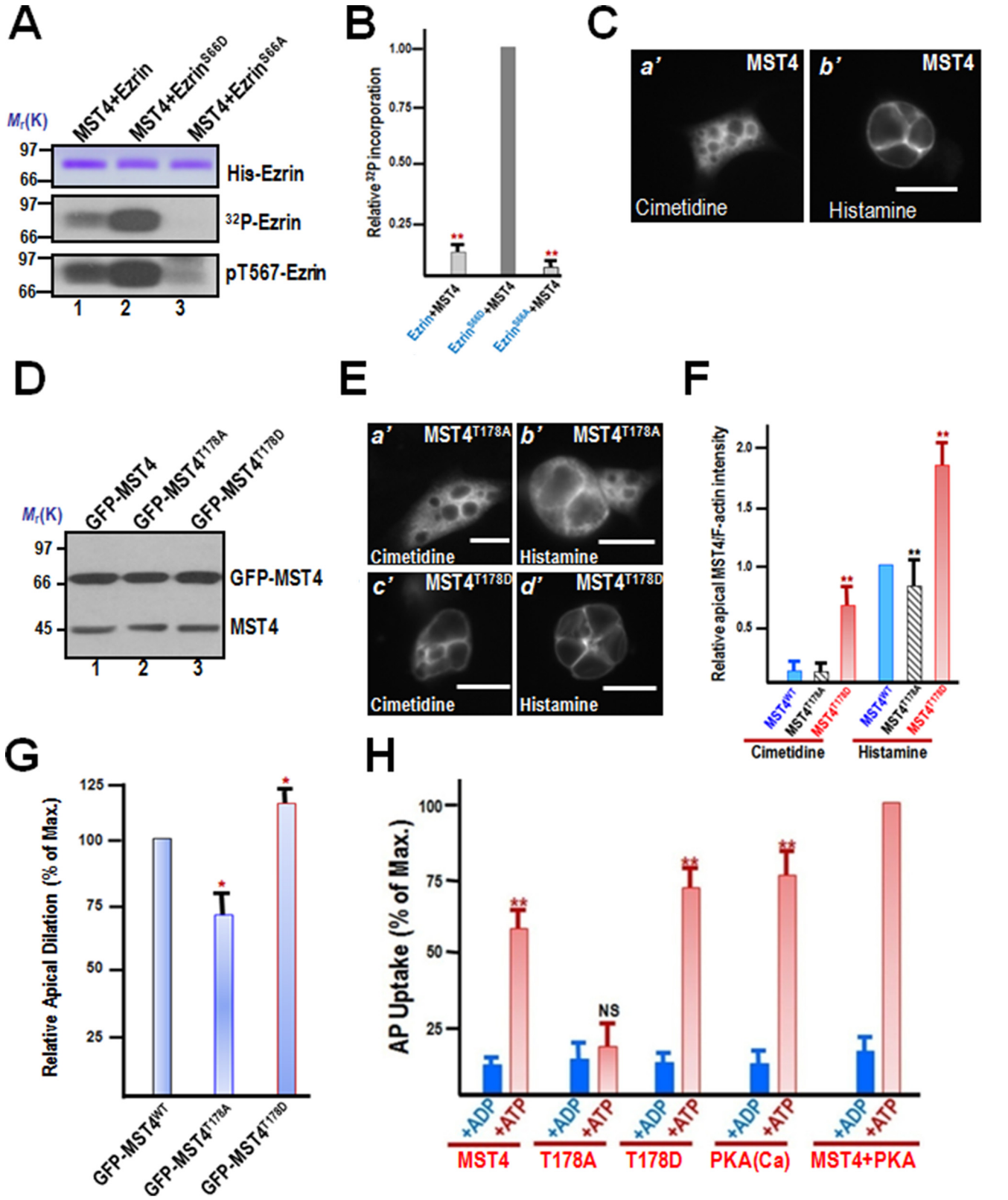

Therefore, we surveyed 100 cells from resting and stimulated populations expressing wild-type MST4, $MST4^{T178A}$, and $MST4^{T178D}$. The vacuolar measurements are summarized in Fig. 4*G*. Histamine stimulation dramatically extended vacuole diameter to 15.9 ± 0.9 μm in control wild-type MST4-expressing parietal cells. However, the average vacuole diameter of histamine-stimulated $MST4^{T178A}$-expressing cells was only 8.9 ± 2.1 μm. We therefore reason that MST4 is essential for the dynamic remodeling of the apical cytoskeleton of parietal cells associated with the stimulation.

The functional importance of MST4 phosphorylation in parietal cell secretion prompted us to examine the precise function of MST4-PKA interaction in parietal cell activation. To directly probe for the function of the PKA-MST4 interaction, we sought to introduce wild-type and mutant MST4 (T178A and T178D) into SLO-permeabilized parietal cells to mimic PKA phosphorylation *in vivo* using a protocol reported previously (16, 18, 19). As predicted, incubation of the recombinant PKA catalytic subunit with MST4 recombinant protein produces an optimal stimulation of acid secretion, as judged by AP uptake (Fig. 4*H*). The $MST4^{T178A}$ mutant inhibited parietal cell secretion, whereas $MST4^{T178D}$ in the absence of exogenous PKA elicited acid secretion equivalent to 74% of maximal stimulation. These results suggest that MST4 cooperates with PKA for maximal parietal cell secretion via phosphorylating ezrin at Ser-66 and Thr-567.

Synergistic Phosphorylation of Ser-66 and Thr-567 for Maximal Secretion in Parietal Cells—Because parietal cell activation is hallmarked by the translocation of H,K-ATPase from tubulovesicles to the apical membrane, we sought to assess the translocation of H,K-ATPase and ACAP4 in non-phosphorylatable ezrin-expressing cells. To this end, cultured rabbit parietal cells were stimulated with histamine, followed by subcellular fractionation and differentiated centrifugation, as illustrated in Fig. 5*A*. A typical panel of Western blot of subcellular fractionation is shown in Fig. 5*B*, in which the histamine-stimulated relocation of H,K-ATPase from the tubulovesicle fraction of P3 to the apical plasma membrane fraction P1 was readily apparent (Fig. 5*B*, *top panel*). ACAP4 is also redistributed to apical plasma membrane fraction P1 from the tubulovesicle fraction of P3 upon histamine stimulation (Fig. 5*B*, *center panel*, *lanes 3* and *4*). Suppression of MST4 via siRNA-mediated knockdown abolished the histamine-elicited relocation of H,K-ATPase (Fig. 5*B*, *top panel*, *lanes 5* and *6*).

To quantify the translocation of ACAP4 and the α subunit of H,K-ATPase in response to histamine stimulation, we carried out densitometric analyses of the α subunit of H,K-ATPase and ACAP4 proteins from P1 (plasma membrane-enriched) and P3 (tubulovesicle-enriched) fractions from resting and secreting rabbit gastric gland preparations and expressed the value as the P1/P3 ratio (Fig. 5*C*). Quantification of the α subunit of H,K-ATPase exhibits a characteristic translocation typically seen in histamine-stimulated, secreting parietal cells (16).

To test whether $ezrin^{S66D/T567D}$ is sufficient to sustain H,K-ATPase relocation, we performed the aforementioned fractionation experiment using cultured parietal cells infected with adenoviral mCherry-ezrin (wild-type, S66D/T567D) after suppression of endogenous MST4 via siRNA-mediated knockdown, followed by histamine stimulation. As shown in Fig. 5*B* and as quantified in Fig. 5*C*, expression of $ezrin^{S66D/T567D}$ in the absence of MST4 was able to sustain the translocation of H,K-ATPase (*, $p < 0.05$; **, $p < 0.01$) compared with cimetidine treatment. We reason that the phosphorylation of Ser-66 and Thr-567 is essential for translocation of H,K-ATPase to the apical plasma membrane of secreting parietal cells.

To directly test the role of phospho-ezrin in parietal cell activation, we introduced recombinant ezrin proteins into SLO-permeabilized parietal cells to mimic Ser-66 and Thr-567 phosphorylation. As shown in Fig. 5*D*, addition of recombinant $ezrin^{S66D/T567D}$ produced a maximal stimulation of acid secretion, whereas S66D or T567D alone only gave a stimulation equivalent to 74% and 37% of the $ezrin^{S66D/T567D}$-treated preparation, respectively (**, $p < 0.01$; *, $p < 0.05$). Consistent with previous studies, non-phosphorylatable ezrin (S66A and T567A) prevents cAMP-elicited parietal cell secretion. Therefore, we conclude that MST4 cooperates with PKA to orchestrate maximal stimulation of acid secretion.

Discussion

Ezrin, a founding member of the membrane-cytoskeleton linker of the ezrin/radixin/moesin protein family, is essential for the regulated plasma membrane-cytoskeletal dynamics

FIGURE 4. **PKA-primed phosphorylation of Ser-66 promotes the phosphorylation of Thr-567 by MST4.** *A*, MST4 exhibits better efficiency in phosphorylation of ezrin-mimicking Ser-66 phosphorylation *in vitro*. Aliquots of recombinant hexahistidine-tagged ezrin, including wild-type and ezrin mutants (S66A and S66D), were incubated with MST4 as detailed under "Materials and Methods." Top panel, Coomassie Blue-stained SDS-PAGE gel. *Bottom panel*, ^{32}P incorporation from the same gel. The efficiency of MST4-elicited ^{32}P incorporation into ezrin is highest in the $ezrin^{S66D}$ mutant (*lane 2*) and very little in the $ezrin^{S66A}$ mutant (*lane 3*). *B*, quantitative analyses of *in vitro* phosphorylation efficiency of Thr-567 using various ezrin proteins mimicking Ser-66 phosphorylation. **, $p < 0.01$ compared with $Ezrin^{S66D}$. *Error bars* represent the mean ± S.E. of three separate preparations. *C*, immunofluorescence staining of MST4 in non-secreting and secreting culture parietal cells. MST4 is primarily located to the cytoplasm, with a slight concentration at the apical membrane (*a'*). However, after histamine stimulation, the MST4 signal is enriched in dilated apical membrane vacuoles (*b'*). *Scale bar* = 10 μm. *D*, characterization of expression of GFP-MST4 proteins in gastric parietal cells. Aliquots of parietal cells were transiently transfected to express MST4 proteins (wild-type, T178A, and T178D). 24 h after transfection, cell lysates were prepared and fractionated on SDS-PAGE, followed by Western blot analyses with MST4 antibody. Note that the exogenous MST4 proteins expressed 3-fold higher compared with endogenous MST4. *E*, PKA-activated MST4 promotes parietal cell activation by histamine stimulation. Aliquots of parietal cells were transiently transfected to express MST4 proteins (T178A and T178D). 24 h after transfection, the parietal cells were treated with histamine (100 μM) as detailed under "Materials and Methods," followed by fixation and immunofluorescence analyses. Note that the exogenous $MST4^{T178D}$-expressing cells exhibited larger apical membrane vacuoles even before histamine stimulation (*c'*). *Scale bars* = 10 μm. *F*, quantitative analyses of apical localization of MST4 (WT; phospho-mimicking, T178D; non-phosphorylatable, T178A) in cimetidine- and histamine-treated parietal cells. **, $p < 0.01$ compared with wild-type MST4-expressing cells in secreting and non-secreting status. *Error bars* represent the mean ± S.E. of three separate preparations of 20 cells in each category. *G*, quantitative analyses of apical vacuole diameter of MST4-expressing parietal cells as a function of activation. *, $p < 0.05$ compared with stimulated controls. *Max.*, maximal stimulation. *Error bars* represent the mean ± S.E. of three separate preparations of 50 cells in each category. *H*, MST4 cooperates with PKA for optimal parietal cell activation. Aliquots of gastric glands were permeabilized with SLO, and various MST4 recombinant proteins and PKA were added to the permeable cells for secretory activity measurements using the AP uptake assay, as described under "Materials and Methods." *NS*, no significant difference; **, $p < 0.001$; *, $p < 0.05$ compared with stimulated controls. *Error bars* represent the mean ± S.E. of three separate preparations.

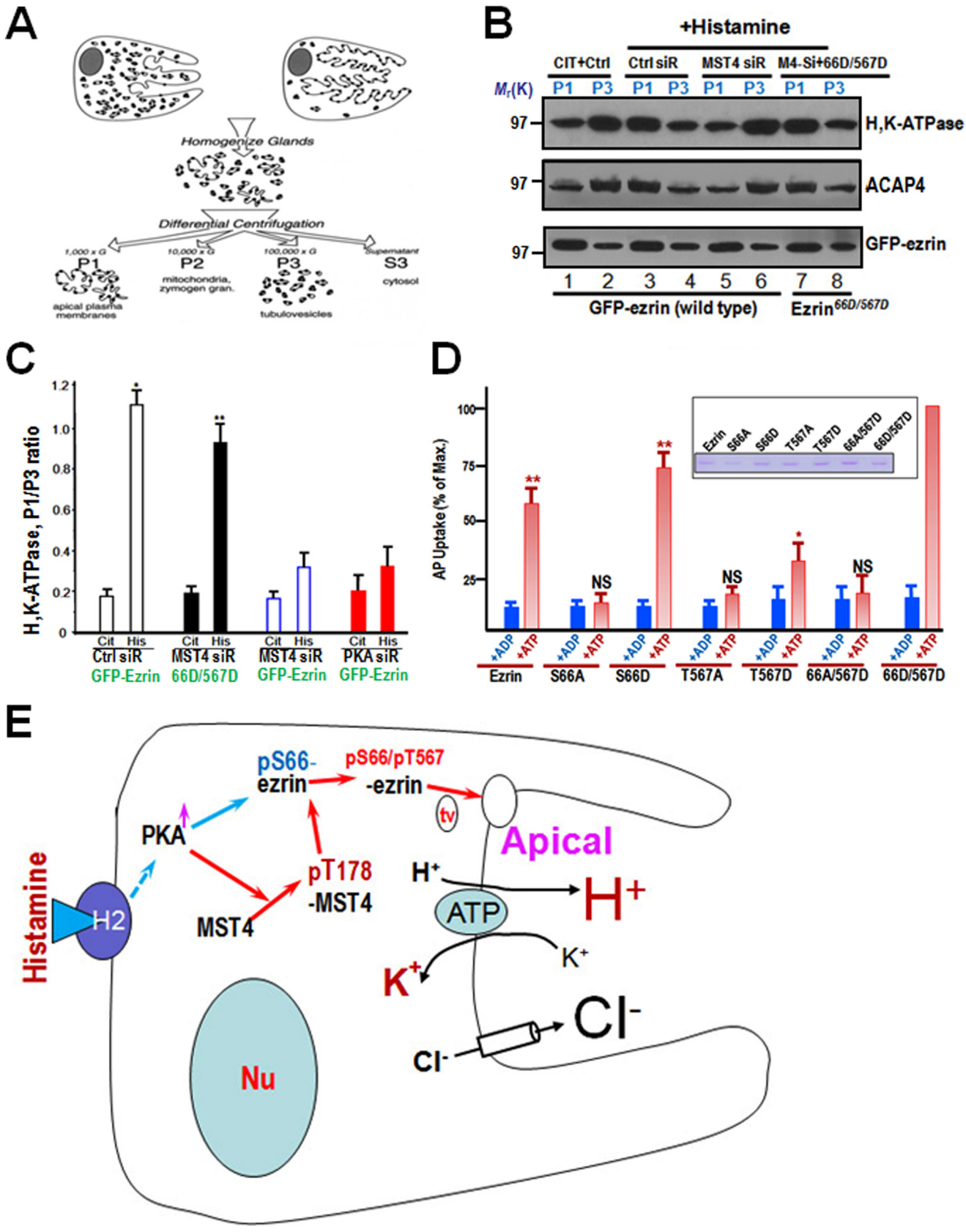
A
Homogenize Glands
Differential Centrifugation
1,000 x G
P1
apical plasma membranes
10,000 x G
P2
mitochondria, zymogen gran.
100,000 x G
P3
tubulovesicles
Supernatant
S3
cytosol
B
+Histamine
CIT+Ctrl
Ctrl siR
MST4 siR
M4-Si+66D/567D
Mr(K)
P1 P3 P1 P3 P1 P3 P1 P3
97
H,K-ATPase
97
ACAP4
97
GFP-ezrin
1 2 3 4 5 6 7 8
GFP-ezrin (wild type)
Ezrin66D/567D
C
H,K-ATPase, P1/P3 ratio
Cit His
Ctrl siR
GFP-Ezrin
MST4 siR
66D/567D
MST4 siR
GFP-Ezrin
PKA siR
GFP-Ezrin
D
AP Uptake (% of Max.)
Ezrin
S66A
S66D
T567A
T567D
66A/567D
66D/567D
NS
+ADP
+ATP
E
Histamine
H2
PKA
pS66-ezrin
pS66/pT567-ezrin
tv
Apical
pT178-MST4
MST4
H+
ATP
K+
Cl-
Nu

underlying cell migration, immunological synapse formation, and polarized secretion (2, 21). Here we provide the first evidence that PKA phosphorylates MST4 at Thr-178, which synergizes the phosphorylation of ezrin at Ser-66 and Thr-567 during parietal cell activation by histamine. This phosphorylation promotes MST4 enzymatic activity by increasing its affinity with substrate and better efficiency in ATP catalysis. The PKA-MST4-ezrin signaling axis is important for parietal cell activation. Therefore, our data provide direct evidence for a phosphorylation-coupled molecular switch of ezrin in orchestrating apical membrane reorganization during regulated secretion (Fig. 5*E*).

During epithelial cell polarization, cells specify their functional domains at the apical and basolateral membrane. The LKB1-STRAD-MO25 complex exhibits an essential role in epithelial cell polarity establishment (22). MST4, as an interactor of the LKB1-STRAD-MO25 complex, specifically controls the formation of brush borders at the apical domain but exhibits no effect on polarization *per se* (15). A recent study has shown that MST4 phosphorylates ezrin at Thr-567, by which MST4 promotes brush border structure establishment. However, MST4 plays no role in the localization of ezrin to the apical membrane, suggesting that another mechanism specifies the localization of ezrin at the apical membrane. Interestingly, MST4 translocates to the apical membrane in response to histamine stimulation because of the recruitment of the vesicular membrane. Although the phosphorylation of MST4 by PKA is essential for its optimal kinase activity, non-phosphorylatable MST4-S178A was also able to enrich at the apical membrane in response to histamine stimulation. Because ezrin is constitutively localized to the apical membrane, the interaction of ezrin with MST4, regardless of its phosphorylation at Thr-178, may account for this PKA phosphorylation-independent apical localization.

Gastric ezrin was initially identified as a PKA substrate associated with parietal cell acid secretion (23). Our recent study has demonstrated that ezrin couples PKA-mediated phosphorylation to the remodeling of the apical membrane cytoskeleton associated with acid secretion in parietal cells (3). However, the mechanism of action underlying ezrin-elicited parietal cell activation by histamine stimulation was less characterized. Our recent study has shown that Ser(P)-66 provides a spatiotemporal cue for tubulovesicle membrane trafficking to the apical membrane via a site-specific phosphorylation-coupled ezrin-Stx3 interaction (13). It is worth noting that ezrin is an interacting protein of the regulatory subunit of PKA that is implicated in the apical localization of PKA (24). Therefore, the interaction between phospho-ezrin and Stx3, established together with an ezrin-ACAP4 interaction characterized previously, may organize an apical signaling, docking, and anchoring complex that orchestrates vesicular membrane recruitment and membrane cytoskeletal reorganization. Further fine mapping of the respective binding interfaces between the aforementioned proteins will aid in delineating the molecular mechanisms underlying polarity establishment and polarized secretion in gastric parietal cells. In addition, it would be of great interest to visualize the spatiotemporal dynamics of MST4 kinase activity in response to histamine stimulation using a FRET-based optical sensor (25). It would be equally important to see how MST4 translocation to the apical membrane responds to its posttranslational modification.

Phosphorylation of ezrin has been functionally linked to membrane dynamics and plasticity. Our early study has demonstrated that persistent phosphorylation of the conserved Thr-567 residue of ezrin alone alters the physiology of gastric parietal cell polarity (26), and this persistent phosphorylation also participates in hepatocarcinoma metastasis (27). We have recently established a protocol in which phosphorylation-mediated protein conformational change can be studied at the single-molecule level using atomic force microscopy (17). Using this protocol, we correlated the phosphorylation-induced conformational change of ezrin-Thr-567 with its functional activity in cellular localization. Using the same protocol, we show that phosphorylation of ezrin at Ser-66 also unfolds ezrin intramolecular association. Future studies will be directed to see how single molecule of ezrin is unfolded in real time in response to PKA and MST4 phosphorylation. It would be equally important to carry out fine comparative analyses using photoactivation localization microscopy to delineate how phosphorylation-coupled protein conformational change is used as a signaling scaffold to orchestrate cellular dynamics (28, 29).

Proper signal transmission by protein kinases requires that they phosphorylate specific substrates at defined sites. It was surprising and exciting to see that PKA phosphorylates MST4 and promotes its catalytic activity, as judged by a dramatically increased k_{cat}/K_m ratio. It would be of great interest to illustrate how phosphorylation of Thr-178 promotes MST4 kinase activity toward ezrin, which is prephosphorylated at Ser-66. This will involve the precise determination of MST4-ezrin structures in phosphorylated and unphosphorylated states. Given

FIGURE 5. **Coordinated phosphorylation of ezrin by PKA and MST4 synergizes histamine-elicited parietal cell secretion.** *A*, schematic of subcellular fractionation used to determine H,K-ATPase-containing tubulovesicle translocation. *B*, Western blot analyses of ezrin, ACAP4, and H,K-ATPase (α subunit) of subcellular fractions derived from resting and stimulated gastric glands infected with mCherry-ezrin adenovirus (wild-type and ezrin$^{S66D/T567D}$) and treated with MST4 siRNA. *CIT*, cimetidine; *Ctrl*, control. *C*, quantitative analyses of the α subunit of H,K-ATPase and ACAP4 proteins from P1 (plasma membrane-enriched) and P3 (tubulovesicle-enriched) fractions. The measurements are expressed as the P1/P3 ratio. Error bars show the mean ± S.E. of four preparations. *Cit*, cimetidine; *His*, histamine. *D*, phosphorylation of Ser-66 and Thr-567 synergized for parietal cell secretion. Gastric glands were SLO-permeabilized and incubated with various recombinant ezrin mutants mimicking Ser-66/Thr-567 phosphorylation independently or in combination before being stimulated with 100 μM cAMP plus 100 μM ATP, and the AP uptake was measured as described under "Materials and Methods." AP data were plotted as a percentage of the stimulated control for each experiment. *Error bars* represent mean ± S.E. ($n = 5$). **, $p < 0.01$; *, $p < 0.05$; *NS*, no significant difference from stimulated controls. Note that the ezrin mutant mimicking both Ser-66 and Thr-567 phosphorylation exhibits the greatest secretory activity in response to cAMP stimulation. *E*, working model illustrating that histamine stimulation signaling induces ezrin conformational change by PKA-elicited phosphorylation of Ser-66, which enables the association of ezrin with tubulovesicle proteins such as ACAP4/syntaxin 3 and provides a spatial cue for tubulovesicle translocation. In non-secreting parietal cells, Stx3 resides on tubulovesicle and relocates apically upon histamine stimulation. Histamine stimulation also induces MST4 phosphorylation at Thr-178 and thus promotes its kinase activity. Phosphorylation of Ser-66 elicits a conformational change of ezrin, which promotes a concurrent phosphorylation of Thr-567 by PKA-activated MST4 to strengthen the linkage of ezrin with actin filaments.

the fact that persistent phosphorylation of Thr-567 of ezrin alters the cellular plasticity in gastric parietal cells and liver cells, it would be of great interest to uncover the phosphatase responsible for reversible dephosphorylation of ezrin, which would serve as a molecular mechanism coordinating parietal cell secreting and resting cycle because persistent acid secretion leads to digestive abnormalities, such as peptic ulcers and *Helicobacter pylori* infection.

Aberrant acid secretion has been seen in the development of peptic ulcers, and correction of aberrant acid production promotes the recovery of patients from peptic ulcers. The current regimens aim for pharmacological inhibitors to block histamine binding to the histamine type 2 receptor or inhibiting proton pump activity. The importance of MST4 kinase activity for optimal acid secretion in parietal cells established here provides insights into better management of aberrant acid secretion using MST4 pharmacological inhibitors. Along this line, it would be exciting to examine whether MST4 kinase is hyperactivated and hyper-phosphorylated in gastric parietal cells of peptic ulcer patients.

Taken together, this work reveals that PKA interacts and phosphorylates the polarity determinant MST4. The phosphorylation of MST4 at Thr-178 promotes its kinase activity and its association with ezrin prephosphorylated at Ser-66. Finally, we show that phosphorylation of Ser-66 by PKA cooperates with the MST4-elicited phosphorylation of Thr-567 on ezrin, which promotes the recruitment of tubulovesicles to the apical membrane and concurrent membrane-cytoskeletal reorganization essential for H,K-ATPase insertion into the plasma membrane. We propose that PKA-MST4 orchestrates the phosphorylation-coupled conformation change of ezrin and provides a spatial control for H,K-ATPase docking at the apical membrane of gastric parietal cells.

Author Contributions—X. L. and X. Y. conceived the project. H. J., W. W., Y. Z., W. W. Y., and F. L. designed and performed most biochemical experiments. W. W., B. Q., X. L., W. Y. Y., T. L. W., and X. D. designed and performed cell biological characterization. H. J., W. W., J. J., C. W. C., H. W., L. L., F. L., and X. D. performed *in vitro* reconstitution experiments and data analyses. All authors contributed to the writing or editing of the manuscript.

Acknowledgments—We thank the members of our groups for discussions.

References

1. Yao, X., and Forte, J. G. (2003) Cell biology of acid secretion by the parietal cell. *Annu. Rev. Physiol.* **65,** 103–131
2. Bretscher, A., Edwards, K., and Fehon, R. G. (2002) ERM proteins and merlin: integrators at the cell cortex. *Nat. Rev. Mol. Cell Biol.* **3,** 586–599
3. Zhou, R., Cao, X., Watson, C., Miao, Y., Guo, Z., Forte, J. G., and Yao, X. (2003) Characterization of protein kinase A-mediated phosphorylation of ezrin in gastric parietal cell activation. *J. Biol. Chem.* **278,** 35651–35659
4. Nakamura, F., Amieva, M. R., and Furthmayr, H. (1995) Phosphorylation of threonine 558 in the carboxyl-terminal actin-binding domain of moesin by thrombin activation of human platelets. *J. Biol. Chem.* **270,** 31377–31385
5. Yao, X., Chaponnier, C., Gabbiani, G., and Forte, J. G. (1995) Polarized distribution of actin isoforms in gastric parietal cells. *Mol. Biol. Cell* **6,** 541–557
6. Yao, X., Cheng, L., and Forte, J. G. (1996) Biochemical characterization of ezrin-actin interaction. *J. Biol. Chem.* **271,** 7224–7229
7. Hanzel, D. K., Urushidani, T., Usinger, W. R., Smolka, A., and Forte, J. G. (1989) Immunological localization of an 80-kDa phosphoprotein to the apical membrane of gastric parietal cells. *Am. J. Physiol.* **256,** G1082–1089
8. Tamura, A., Kikuchi, S., Hata, M., Katsuno, T., Matsui, T., Hayashi, H., Suzuki, Y., Noda, T., Tsukita, S., and Tsukita, S. (2005) Achlorhydria by ezrin knockdown: defects in the formation/expansion of apical canaliculi in gastric parietal cells. *J. Cell Biol.* **169,** 21–28
9. Zhu, L., Zhou, R., Mettler, S., Wu, T., Abbas, A., Delaney, J., and Forte, J. G. (2007) High turnover of ezrin T567 phosphorylation: conformation, activity, and cellular function. *Am. J. Physiol. Cell Physiol.* **293,** C874–884
10. Peng, X. R., Yao, X., Chow, D. C., Forte, J. G., and Bennett, M. K. (1997) Association of syntaxin 3 and vesicle-associated membrane protein (VAMP) with H^+/K^+-ATPase-containing tubulovesicles in gastric parietal cells. *Mol. Biol. Cell* **8,** 399–407
11. Karvar, S., Yao, X., Duman, J. G., Hybiske, K., Liu, Y., and Forte, J. G. (2002) Intracellular distribution and functional importance of vesicle-associated membrane protein 2 in gastric parietal cells. *Gastroenterology* **123,** 281–290
12. Karvar, S., Yao, X., Crothers, J. M., Jr., Liu, Y., and Forte, J. G. (2002) Localization and function of soluble *N*-ethylmaleimide-sensitive factor attachment protein-25 and vesicle-associated membrane protein-2 in functioning gastric parietal cells. *J. Biol. Chem.* **277,** 50030–50035
13. Yu, H., Zhou, J., Takahashi, H., Yao, W., Suzuki, Y., Yuan, X., Yoshimura, S. H., Zhang, Y., Liu, Y., Emmett, N., Bond, V., Wang, D., Ding, X., Takeyasu, K., and Yao, X. (2014) Spatial control of proton pump H,K-ATPase docking at the apical membrane by phosphorylation-coupled ezrin-syntaxin 3 interaction. *J. Biol. Chem.* **289,** 33333–33342
14. Rawat, S. J., and Chernoff, J. (2015) Regulation of mammalian Ste20 (Mst) kinases. *Trends Biochem. Sci.* **40,** 149–156
15. ten Klooster, J. P., Jansen, M., Yuan, J., Oorschot, V., Begthel, H., Di Giacomo, V., Colland, F., de Koning, J., Maurice, M. M., Hornbeck, P., and Clevers, H. (2009) Mst4 and Ezrin induce brush borders downstream of the Lkb1/Strad/Mo25 polarization complex. *Dev. Cell* **16,** 551–562
16. Ammar, D. A., Zhou, R., Forte, J. G., and Yao, X. (2002) Syntaxin 3 is required for cAMP-induced acid secretion: streptolysin *O*-permeabilized gastric gland model. *Am. J. Physiol. Gastrointest. Liver Physiol.* **282,** G23–33
17. Liu, D., Ge, L., Wang, F., Takahashi, H., Wang, D., Guo, Z., Yoshimura, S. H., Ward, T., Ding, X., Takeyasu, K., and Yao, X. (2007) Single-molecule detection of phosphorylation-induced plasticity changes during ezrin activation. *FEBS Lett.* **581,** 3563–3571
18. Wang, F., Xia, P., Wu, F., Wang, D., Wang, W., Ward, T., Liu, Y., Aikhionbare, F., Guo, Z., Powell, M., Liu, B., Bi, F., Shaw, A., Zhu, Z., Elmoselhi, A., Fan, D., Cover, T. L., Ding, X., and Yao, X. (2008) *Helicobacter pylori* VacA disrupts apical membrane-cytoskeletal interactions in gastric parietal cells. *J. Biol. Chem.* **283,** 26714–26725
19. Ding, X., Deng, H., Wang, D., Zhou, J., Huang, Y., Zhao, X., Yu, X., Wang, M., Wang, F., Ward, T., Aikhionbare, F., and Yao, X. (2010) Phospho-regulated ACAP4-Ezrin interaction is essential for histamine-stimulated parietal cell secretion. *J. Biol. Chem.* **285,** 18769–18780
20. Cao, X., Ding, X., Guo, Z., Zhou, R., Wang, F., Long, F., Wu, F., Bi, F., Wang, Q., Fan, D., Forte, J. G., Teng, M., and Yao, X. (2005) PALS1 specifies the localization of ezrin to the apical membrane of gastric parietal cells. *J. Biol. Chem.* **280,** 13584–13592
21. Fehon, R. G., McClatchey, A. I., and Bretscher, A. (2010) Organizing the cell cortex: the role of ERM proteins. *Nat. Rev. Mol. Cell Biol.* **11,** 276–287
22. Baas, A. F., Kuipers, J., van der Wel, N. N., Batlle, E., Koerten, H. K., Peters, P. J., and Clevers, H. C. (2004) Complete polarization of single intestinal epithelial cells upon activation of LKB1 by STRAD. *Cell* **116,** 457–466
23. Urushidani, T., Hanzel, D. K., and Forte, J. G. (1989) Characterization of an 80-kDa phosphoprotein involved in parietal cell stimulation. *Am. J. Physiol.* **256,** G1070–1081
24. Dransfield, D. T., Bradford, A. J., Smith, J., Martin, M., Roy, C., Mangeat, P. H., and Goldenring, J. R. (1997) Ezrin is a cyclic AMP-dependent protein kinase anchoring protein. *EMBO J.* **16,** 35–43
25. Chu Y, Yao PY, Wang W, Wang D, Wang Z, Zhang L, Huang Y, Ke Y, Ding

X, & Yao X. (2011) Aurora B kinase activation requires survivin priming phosphorylation by PLK1. *J. Mol. Cell Biol.* **3,** 260–267

26. Zhou, R., Zhu, L., Kodani, A., Hauser, P., Yao, X., and Forte, J. G. (2005) Phosphorylation of ezrin on threonine 567 produces a change in secretory phenotype and repolarizes the gastric parietal cell. *J. Cell Sci.* **118,** 4381–4391
27. Chen, Y., Wang, D., Guo, Z., Zhao, J., Wu, B., Deng, H., Zhou, T., Xiang, H., Gao, F., Yu, X., Liao, J., Ward, T., Xia, P., Emenari, C., Ding, X., Thompson, W., Ma, K., Zhu, J., Aikhionbare, F., Dou, K., Cheng, S. Y., and Yao, X. (2011) Rho kinase phosphorylation promotes ezrin-mediated metastasis in hepatocellular carcinoma. *Cancer Res.* **71,** 1721–1729
28. Xia, P., Liu, X., Wu, B., Zhang, S., Song, X., Yao, P. Y., Lippincott-Schwartz, J., and Yao, X. (2014) Superresolution imaging reveals structural features of EB1 in microtubule plus-end tracking. *Mol. Biol. Cell* **25,** 4166–4173
29. Xia P, Zhou J, Song X, Wu B, Liu X, Li D, Zhang S, Wang Z, Yu H, Ward T, Zhang J, Li Y, Wang X, Chen Y, Guo Z, & Yao X. (2014) Aurora A orchestrates entosis by regulating a dynamic MCAK-TIP150 interaction. *J. Mol. Cell Biol.* **6,** 240–254